Proceedings of the 9th International Conference on Physical Modelling in Coastal Engineering (Coastlab24)

Delft, Netherlands, May 13-16, 2024

Conference Paper, DOI: 10.59490/coastlab.2024.702

STUDY OF THE EFFECT OF SPUR DIKES ON BEACH PROTECTION BASED ON PHYSICAL MODEL EXPERIMENT

FUYUAN CHEN[1,2], ZHIGUO HE[2], HE KUN[1], WANG QIUSHUN[1]

1.Zhejiang institute of Hydraulics & Estuary,

2.Zhejiang University

ABSTRACT

The Qiantang River is a typical strong tide estuary, the world-famous tidal bore have huge turbulent energy and causes damage to the sea wall. Spur dike is an important engineering to prevent the seawall foundation from tidal bore. But the tidal bore occurs at the low tide level, strong turbulence, high flow velocity, water level rises sharply. The spur dike height, length, inclination angle need to be determined by physical model according to the specific bore dynamic conditions. In the tests, the fixed-bed model was used to study the tidal current velocity reduction rate and region, the falling current circulation characteristics in dike field. The movable-bed model test is used to study the effect of each test on protecting the beach. This physical model study reveals the rule of spur dike influence on tidal bore dynamics so the effect of spur dike on protecting the beach is clear.

KEYWORDS: Spur Dike, Tidal Estuary, Physical Model

1 INTRODUCTION

The Qiantang River is a typical macro-tidal estuary, with tidal waves reaching the section above Ganpu. The effect of the shallow water deformation is intensified, forming a spectacular tidal bore that propagates upwards for more than 100 km. Tidal bores have strong turbulent effect, which the swirling and breaking of the tidal bore front cause the dissipation of huge energy. It rapidly erodes the riverbed, causing great damage to structures such as seawalls, which is one of the main factors causing the damage of seawalls in the Qiantang River Estuary.

Recently, extensive researches have been conducted by many scholars on the effect of spur dikes on the beach protection under unidirectional currents [1-6], but the dynamic conditions of tidal bores in river bends lead to extremely complex hydrodynamics due to the presence of spur dikes. However, there is relatively little research on the effect of dikes on the beach protection. The hydraulic characteristics of tidal bores are different from the unidirectional flows. Tidal bores are generally accompanied by strong currents with rotational and broken mass waves. There are remarkable three-dimensional turbulent characteristics of the tidal bore front. When it directly acts on the riverbed or beach, sediment particles will be easily suspended due to the strong lifting effect. Sediment concentration in the tidal bore front can reach up to 45 kg/m3. After the passage of tidal bores, the water level rises sharply by 2-3 m, and then the subsequent strong current of tidal bores, i.e.fast-moving water, can reach up to 6-10 m/s, which maintains the strong capabilities of sediment transport and erosion. After being subjected to the action of spur dikes, the water level further rises, and the root of spur dikes is susceptible to be eroded. The flow of tidal bores over spur dikes will erode the upstream reach, and tidal currents are influenced by spur dikes, which generates strong three-dimensional flow around the head of dikes. It causes severe erosion of the riverbed and the scouring holes at the head of dikes are formed. Therefore, it is necessary to investigate the effect of spur dikes on the beach protection under the dynamic conditions of tidal bores through physical models due to the great uncertainty of the effects.

2 ENVIRONMENTAL CONDITIONS IN STUDY SITES

The Jianshan river bay is controlled by the convex on the north bank of the Qiantang River, and the effect of river bend is obvious. The tide from Hangzhou Bay flowing upstream into the Jianshan River reach is divided into two parts, i.e. south and north tidal bores. The southern tidal bores propagate upstream from the southern seawall, while the northern tidal bores are obliquely intersected with the southern seawall. Consequently, the two types of tidal bores act together on the southern seawall. The numerical results of the two types of tidal bores acting on the southern shore of Jianshan is shown in Fig.1. Under the action of tidal bores, the foot of the south bank seawall is severely eroded. Figure 2 demonstrates the scouring of the foot of the seawall under tidal bores, with sheet piles exposed at a height of over 2 meters.

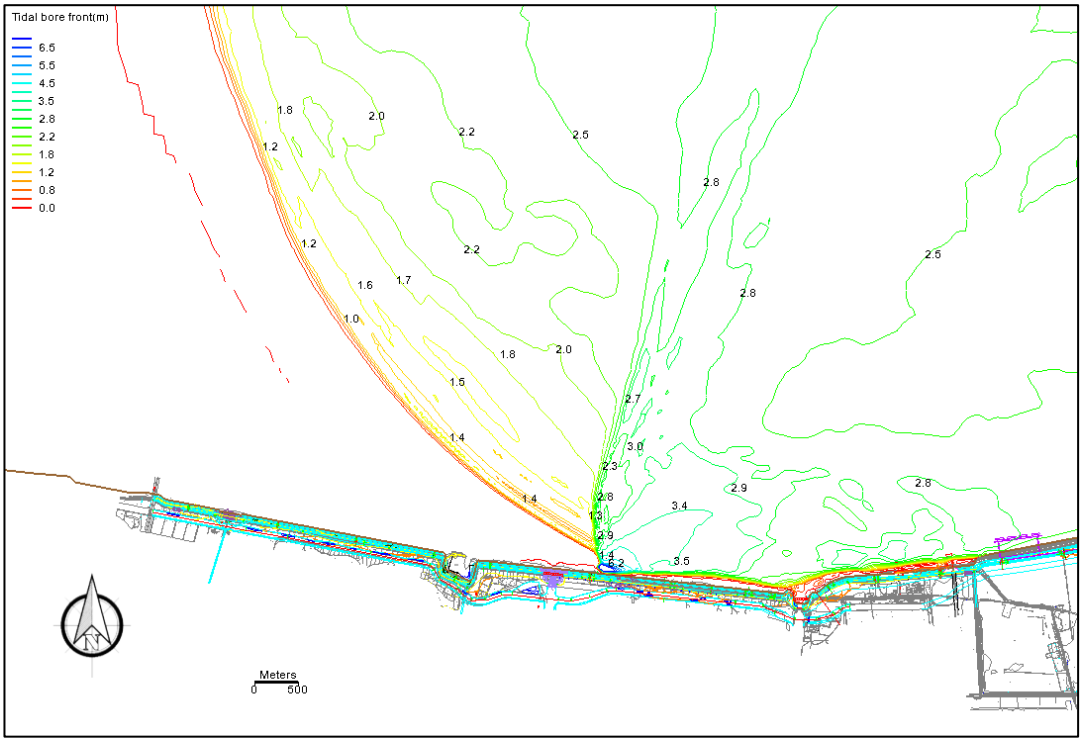

Figure 1. Numerical simulation of north-south tidal bores in the Jianshan reach.

Figure 2. Photo of exposed sheet piles in the south bank scouring seawall.

The main parameters of the layout of the protective dike include the angle between the dike and seawall, the length of the dike, the spacing of the dikes, and the elevation of the dike. After comparing the hydrodynamics results of various spur dike schemes on the basis of numerical results, the more ideal layout scheme of spur dike was determined to be a length of 80 m, an elevation of 1.0 m, and an interval space of 200 m. Therefore, the layouts of 11 spur dikes are shown in Fig. 3. In this study, physical model experiments are used to further verify the reduction of spur dikes by investigating the hydrodynamics, and whether the elevation of the beach area in front of the seawalls can be maintained above the design requirement of -3.0 m.

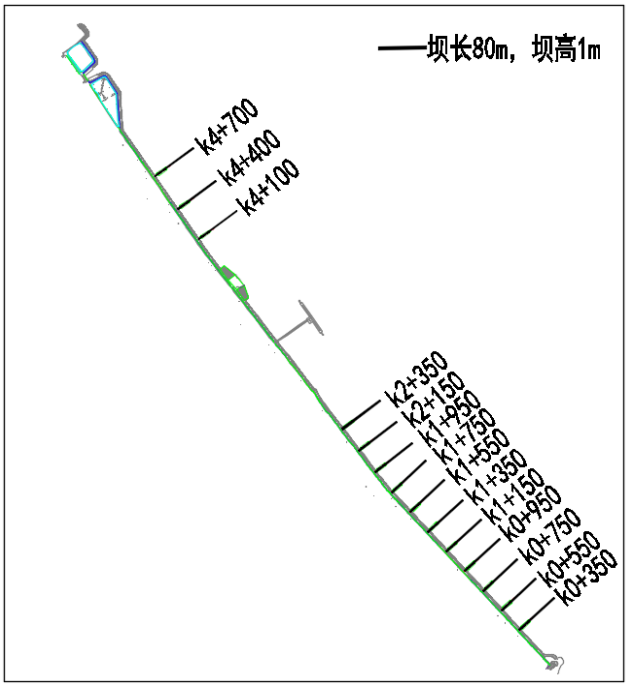

Figure 3. Sketch of the layout of spur dikes.

3 PHYSICAL MODEL

3.1 Physical model

3.1.1. Model range and scale

The total length of the physical model is about 10.4 km, with a simulated water area of 27.0 km^2. The model layout is shown in Fig. 4. Due to the limit of the model site, the transition section of flow inlet, the selection of model sand, and the characteristics of tidal bores in the study area, the horizontal scale of the overall physical model is selected λ_L=200, and the vertical scale λ_H=100. The variation rate of the horizontal and vertical scales η= 2.0. The model terrain takes into account dynamic factors and the volume of the riverbed, the bathymetry with 1:50000 large-scale from July 2018 is employed. Additionally, the refined bathymetry within 200 m in front of the seawall from July to August 2018 is used.

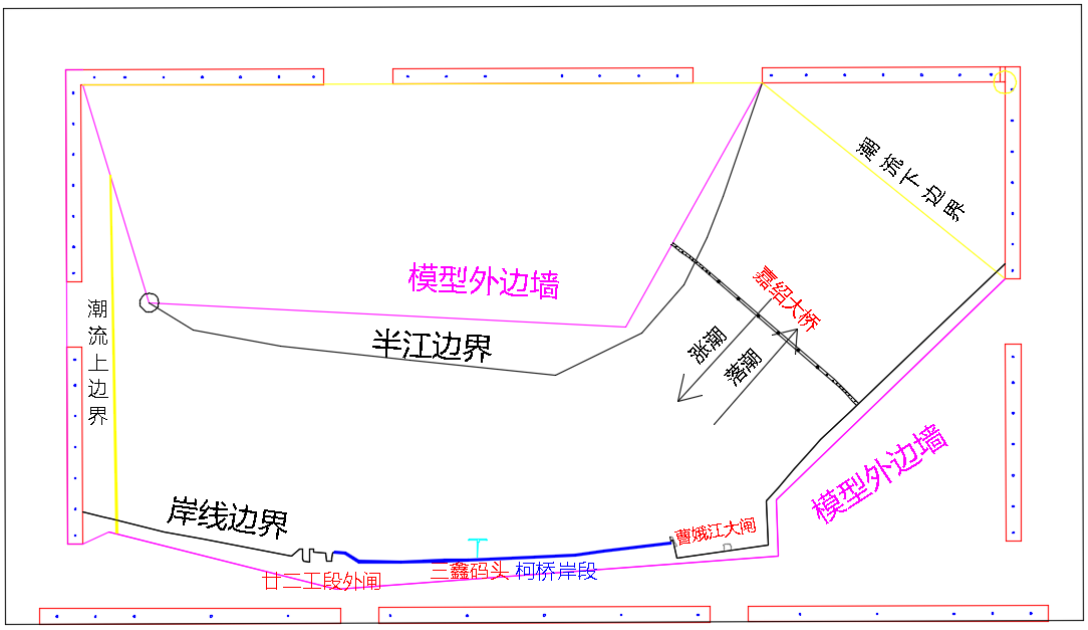

Figure 4. Layout of physical model.

3.1.2. Main similarity conditions

The similarity conditions of geometry, water flow, and sediment movement are satisfied in the model design to simulate water flow and sediment movement. The main similarity of sediment suspension and riverbed deformation is satisfied when simulating sediment movement, in order to meet the similarity of sediment incipience, sediment transport and sediment deposition. The scales of the similarity are listed in Table 1, where the main scales λ_u, λ_ω, λ_{v_c}, λ_t, λ_{nb} represent the scales of the velocity, sediment settling, sediment incipience velocity, water flow time and riverbed roughness.

Table 1. Similarity conditions.

Similarity	Calculated formula	Calculated	Physical model
Horizontal scale	λ_l	250	250
Vertical scale	λ_h	100	100
Velocity scale	$\lambda_u = \lambda_v = \lambda_h^{1/2}$	10	10
Water flow time scale	$\lambda_t = \lambda_l / \lambda_u$	25	25
Riverbed roughness scale	$\lambda_{n_b} = \lambda_h^{2/3} / \lambda_l^{1/2}$	1.36	1.36
Sediment deposition scale	$\lambda_\omega = \frac{\lambda_h}{\lambda_l}\lambda_u$	4	3
Sediment incipience velocity scale	$\lambda_{v_c} = \lambda_u$	10	10.5

3.1.3. The selection of model sand

The main aim of the movable bed model experiment is to study the effect of dikes on preventing erosion, promoting sedimentation, and protecting beach at the foot of seawalls before and after the layout of the dikes. Based on the grading data of suspended load and bed load, the model sand satisfies the similarities of sediment incipience, sediment carrying, while

appropriately considering the settlement similarity requirements of suspended load. The median sizes of sediment particles in the southern bank of Jianshan reach is relatively fine, with a median particle size (d50) ranging from 0.02 to 0.04mm. It belongs to fine silt and has a relatively uniform grading. The difference in particle sizes between bed load and suspended load is not significant. Based on the calculation of theoretical formulas and considering the water depth in the study area, the sediment incipience velocity in the study area is about 0.7 m/s (water depth 5-15 m), and its average settling velocity is about 0.06 cm/s.The riverbed erosion and deposition can be simulated by wood powder materials in the terrain of curved river, and the processes of sediment incipience and sediment deposition are in good agreement with the actual situation. Therefore, it is proposed to choose wood powder materials with a median particle size of 0.07mm as the experimental model sand in the movable bed physical model. The bulk density of this wood powder is 1.09 g/cm3, and the sediment incipience velocity is about 7 cm/s (water depth 5-15 cm), and the settling velocity is about 0.02 cm/s. After comparison with the scale calculation, the average scale of the sediment incipience velocity is about 10.5, and the scale of the sediment deposition is 3. Consequently, it is seen that the sediment incipience velocity of the model sand is relatively consistent with the required value, which basically conforms to the requirements of the movable bed physical model.

3.2. Model validation

3.2.1. The verification of hydrodynamics

The immovable bed model was validated using hydrological data from the spring tide on July 29-30, 2019, which is used to verify the model's ability for reproducing the hydrodynamic characteristics in the study area. The locations of the verification stations in this study are shown in Fig. 5. The upstream and downstream boundaries conditions in the physical model are determined by the large-scale numerical model.

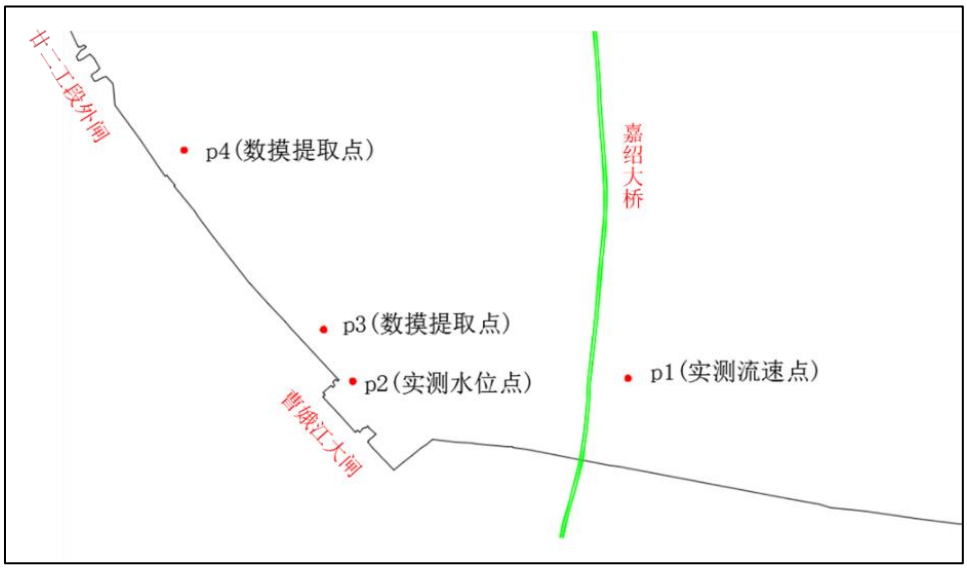

(a) Distribution of measured points

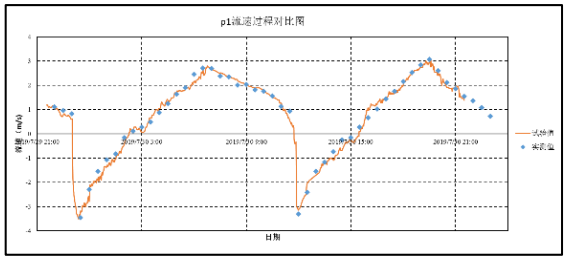

(b) Comparison of velocity at P1

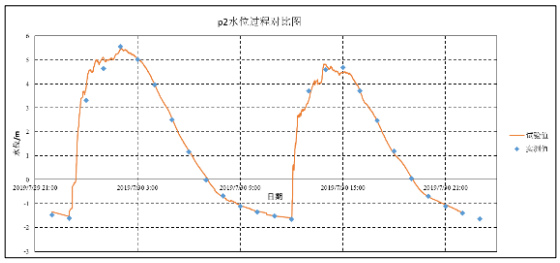

(c) Comparison of water level at P2

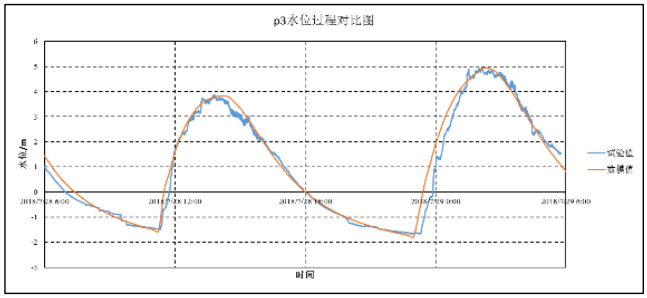

(d) Comparison of water level at P3

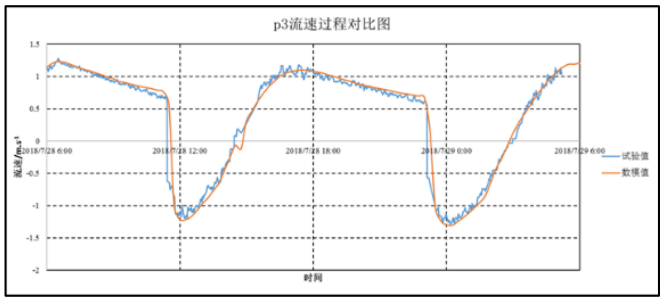

(e) Comparison of velocity at P3

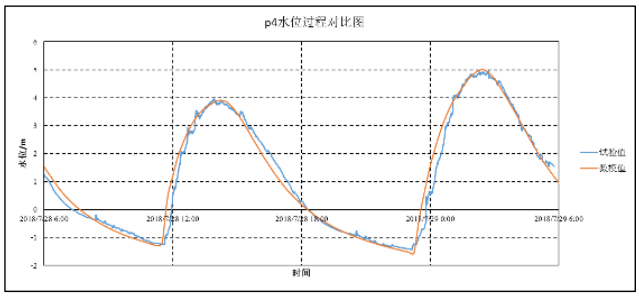

(f) Comparison of water level at P4

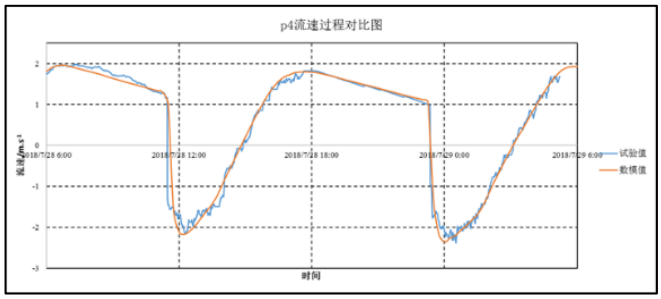

(g) Comparison of velocity at P4

Figure 5. Verification of tidal flow.

3.2.2 Verification of riverbed erosion and sedimentation

The bathymetry data on the left bank of the Cao'e River sluice near the study area in July 2018 are used to validate the movable bed model. In the physical experiment, the dynamic conditions during the spring tide in the July 2018 were applied to the study area, and the results are shown in Fig. 6. The measured deepest point is -7.1 m, and the measured deepest point in the experiment is -7.2 m. It can be seen that the experimental value of the deepest point elevation of the local scouring hole on the convex body is slightly lower than the measured value by 0.1 m. Moreover, both the experimental and measured features are developed along the contour line of the convex body from the morphology of the scouring hole. Due to a certain amount of riprap in front of the convex body during the measurement, the erosion hole and the deepest point are shifted outward.

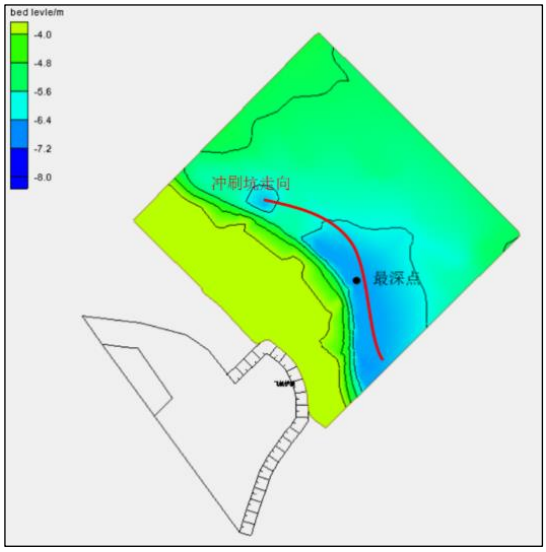

（a）the measured bathymetry

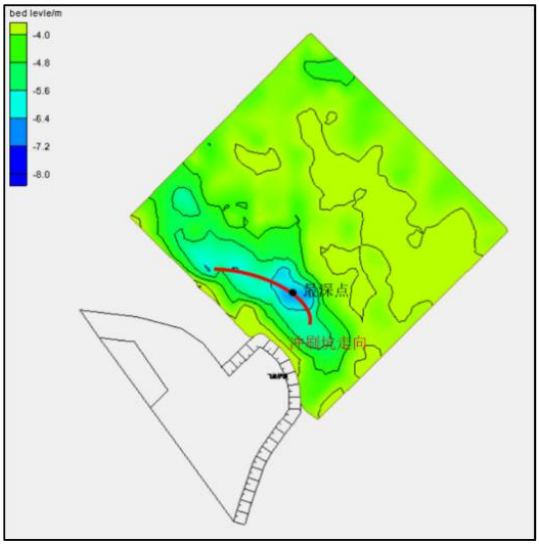

（b）the simulated bathymetry

Figure 6. Verification of the bathymetry between the measured and the physical model.

3.3. Results

A 300 return year spring tide is used as the dynamic boundary in the physical experiment, and the layout of monitoring points of the flow velocity in the scheme is shown in Fig.7. Point 1 is located 200 m offshore, which characterizes the situation of the main channel outside the spur dike. Point 2 is placed 40 m downstream of the first dike and 15 m away from the foot of the seawall, characterizing the situation of the downstream side beach of the dike. The points ranging from 3 # to 6 # are placed at positions 15 m, 30 m, 50 m, and 80 m offshore of the first dike, representing the situation in various parts of the first dike. Points 7 # and 8 # are arranged at a distance of 15 m and 30 m offshore from the middle area between dikes, representing the situation of various parts of the middle area. The points ranging from 9 # to 14 # are placed 15 m offshore within each middle area between dikes, indicating the situation at the foot of the seawall within the dikes.

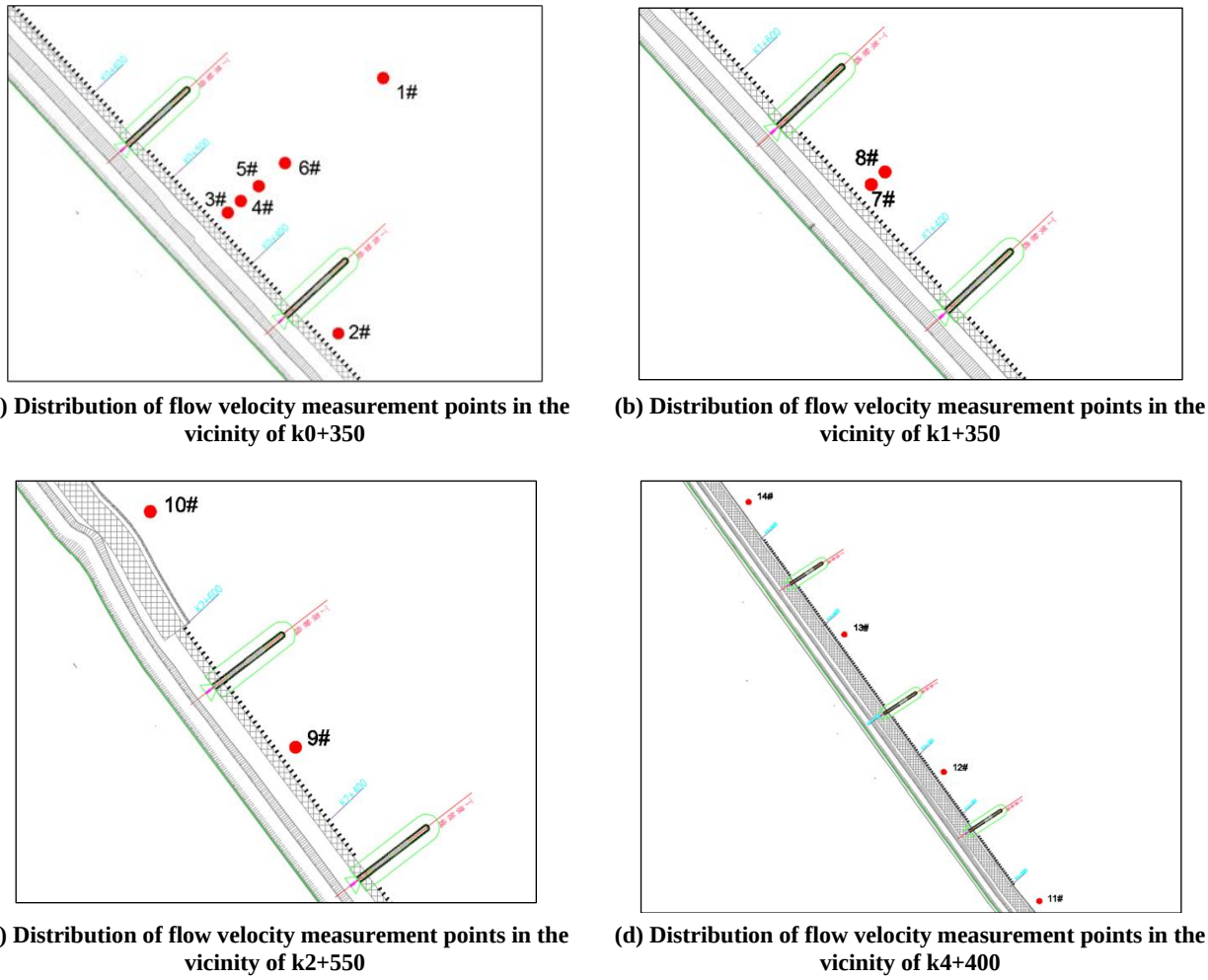

(a) Distribution of flow velocity measurement points in the vicinity of k0+350

(b) Distribution of flow velocity measurement points in the vicinity of k1+350

(c) Distribution of flow velocity measurement points in the vicinity of k2+550

(d) Distribution of flow velocity measurement points in the vicinity of k4+400

Figure 7. Distribution of flow velocity measurement points

3.3.1. Flow reduction

It is seen that the flow velocity in the vicinity of the seawall area slows down significantly after the construction of the dikes according to Table 2 and Fig. 8. During the flood tide, the average reduction of the flood tide velocity at the foot of the seawall in the middle area between dikes is 70%, the average reduction of the flood tide velocity is 56%, and the average reduction rate of the ebb tide velocity is about 64%. In the middle area between dikes, the reduction rate of tidal current velocity decreases when it moves outward. The tidal current velocity has slightly increased outside the cover area of dikes.

Table 2. Statistical table of the changes of tidal flows.

Condition	Maximum flood velocity			Average flood velocity			Maximum ebb velocity		
Scheme / Points	Before spur dikes (m/s)	After spur dikes (m/s)	Change (%)	Before spur dikes (m/s)	After spur dikes (m/s)	Change (%)	Before spur dikes (m/s)	After spur dikes (m/s)	Change (%)
1#	4.5	4.5	1%	2.4	2.4	1%	2	2.1	4%
2#	3.1	1.6	-48%	1.7	1.2	-29%	1.5	0.4	-75%
3#	3.2	1.4	-55%	1.7	1.1	-36%	1.6	0.4	-72%
4#	3.5	0.8	-77%	1.9	0.7	-65%	1.8	0.4	-78%
5#	3.5	1.1	-69%	1.9	0.9	-56%	1.9	0.5	-76%
6#	3.8	1.4	-63%	2.1	1.2	-44%	2	0.7	-63%
7#	4.3	0.8	-81%	2.3	0.7	-69%	1.7	0.4	-79%
8#	4.7	0.8	-83%	2.5	0.6	-74%	1.9	0.4	-78%
9#	4.5	0.8	-82%	2.4	0.6	-75%	1.5	0.3	-83%
10#	4.1	0.8	-82%	2.2	0.6	-72%	1.6	1.3	-21%
11#	4.4	2	-54%	2.3	1.5	-34%	1.1	0.5	-54%
12#	4.6	1.4	-70%	2.4	1.2	-52%	1.3	0.5	-59%
13#	4.4	1.1	-75%	2.4	0.8	-66%	1.1	0.8	-28%
14#	3.6	1.2	-68%	2.0	0.9	-56%	0.9	0.9	-1%

Note: The change is based on the current velocity before constructing spur dikes, with (+) indicating an increase and (-) indicating a decrease.

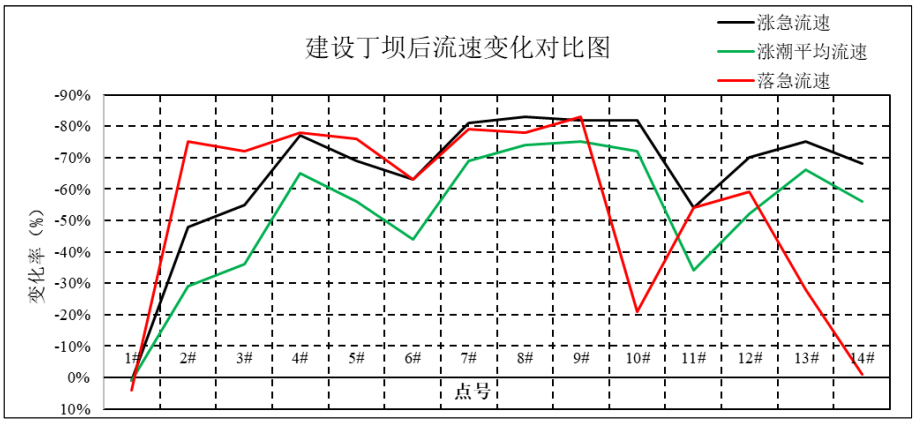

Figure 8. Comparison of flow velocity after the construction of spur dikes.

3.3.2 Flow velocity distribution

The distribution of the flow velocity measured by the surface flow field system is demonstrated in Fig. 9. It is observed that there are also strip shaped flow velocity reduction zones in the vicinity of the seawall after the protection of the dikes. Before the construction of the dikes, the rapid flow velocity of the flood and ebb tides near the seawall area was greater than 3 m/s. After the construction of the dikes, there are a flood velocity of less than 1 m/s, and an ebb velocity of less than 1m/s in more than 60% of the area in the middle area between spur dikes.

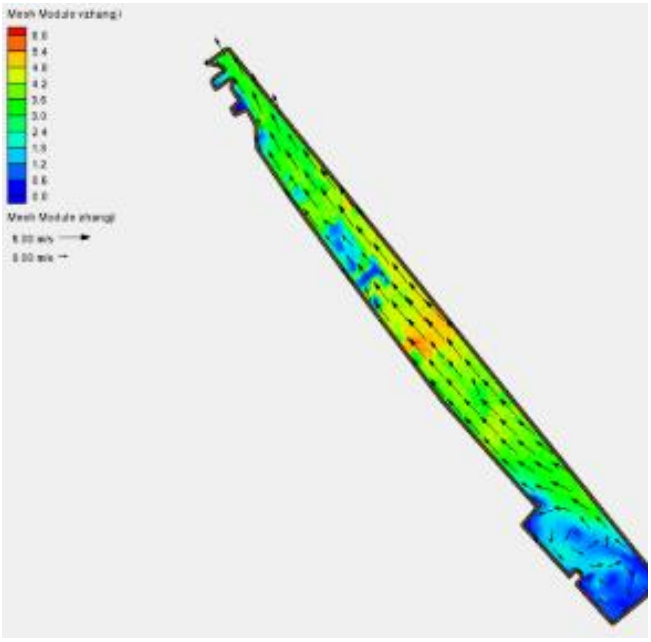

(a)Maximum flood without spur dikes

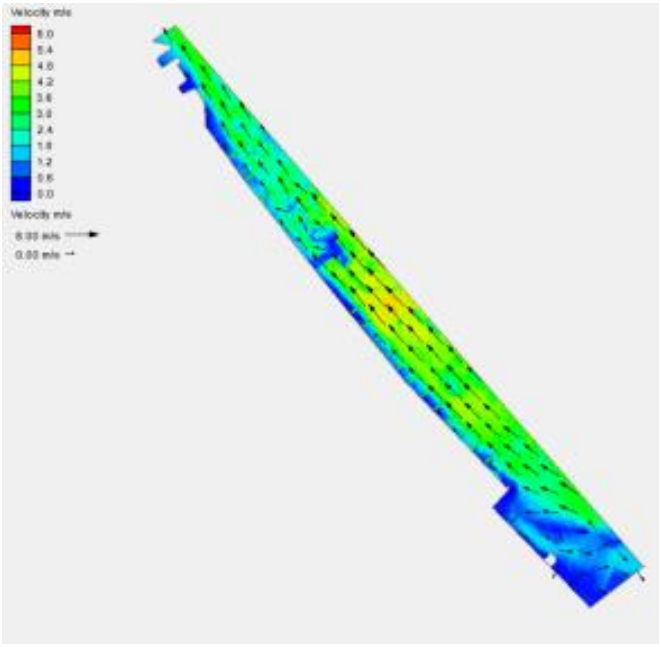

(b) Maximum flood with spur dikes

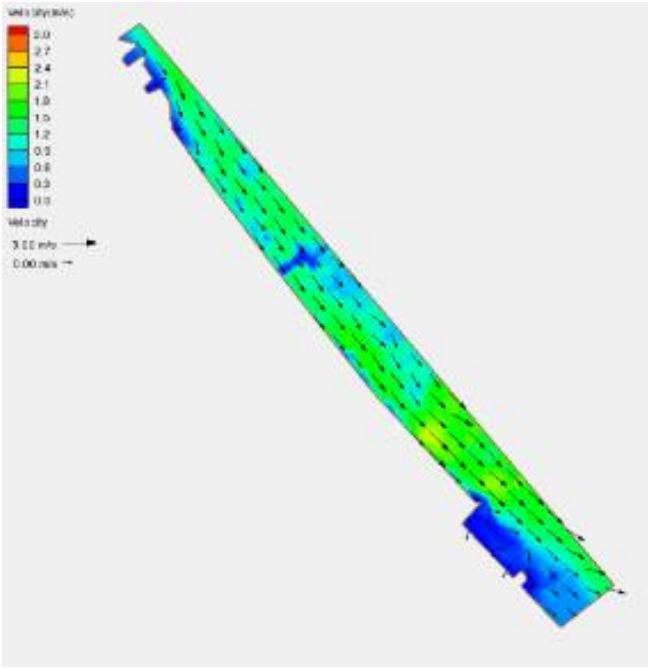

(c)Maximum ebb without spur dikes

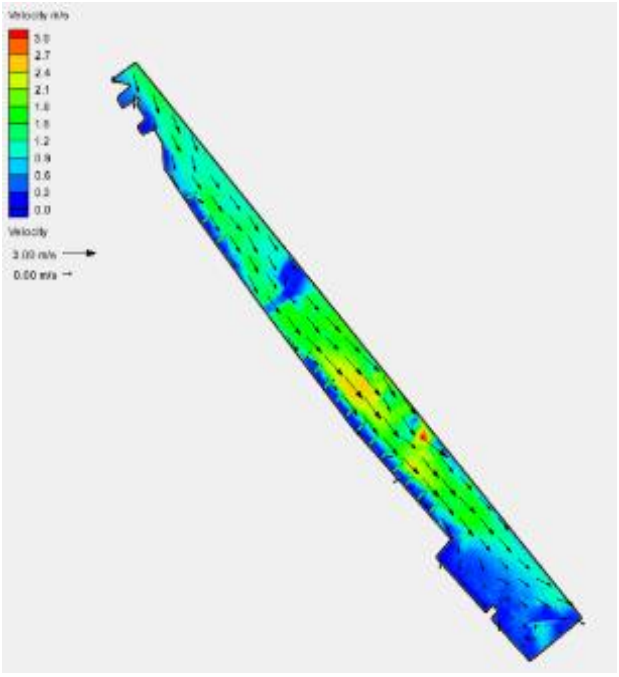

(d) Maximum ebb with spur dikes

Figure 9. Distribution of the flow field under spur dikes.

3.3.3. Circulation distribution

There is a sediment deposition area in the circulation area within the middle area between dikes, which is an important indicator of the strength of the dike's beach protection effect. It can be seen that there is a circulation in the middle area between dikes (Fig.10), which makes it easy for sediment to accumulate and settle, enhancing the beach protection effect.

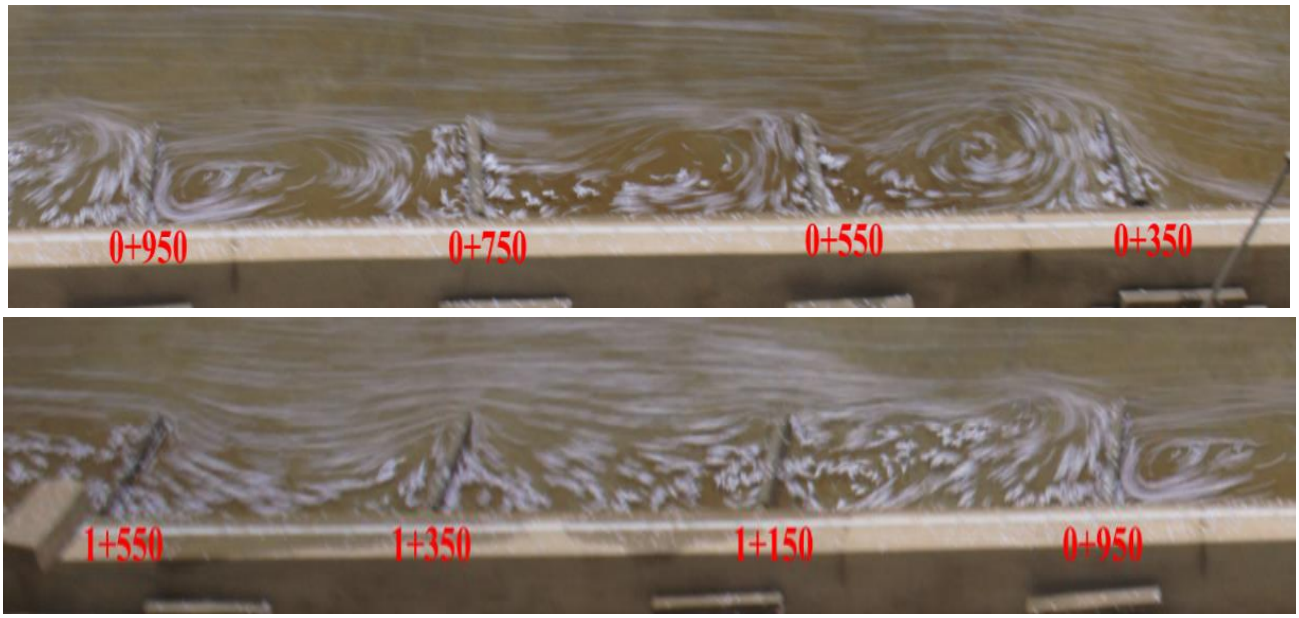

Figure 10. Flow trace after the construction of spur dikes.

3.3.4. Beach protection effect

Figure 11 shows the sedimentation situation in the middle area between dikes. After the construction of the spur dike, the elevation of the beach in the middle area between dikes significantly increased. It is because that the flow velocity of the middle area between dikes was decreased after the construction of the spur dikes, and the sediment carried by the tide was settled by the circulation between the spur dikes. It is seen that the spur dikes have a significant protective effect on the nearshore beach. In the experiment, it is noted that spur dikes are beneficial for sediment deposition in the middle area between dikes, but there are obvious local erosion holes at the the head and the upstream of the spur dike, which will affect the safety of the spur dikes.

Figure 11. Photo of the beach near the seawall after the construction of spur dikes.

From the experimental data, the elevation changes of the beach at 10 m outside the foot of the seawalls are shown in Table 3. It is seen that the sediment deposition elevation of the beach from 1 to 10 is about 2.84 m, and the average sediment deposition elevation of the beach from 11 to 12 is 1.07 m. The elevation of the beach area in front of the seawall is above -4 m, which satisfies the safety and stability requirements of the seawall.

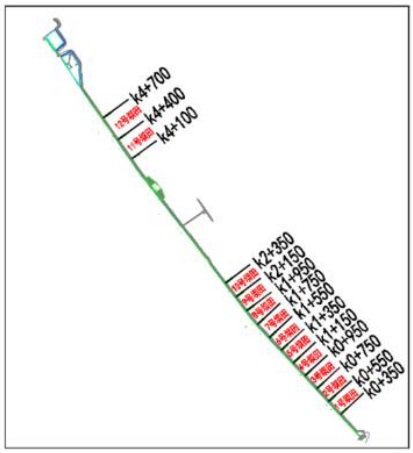

(a)Sketch of the locations of spur dikes

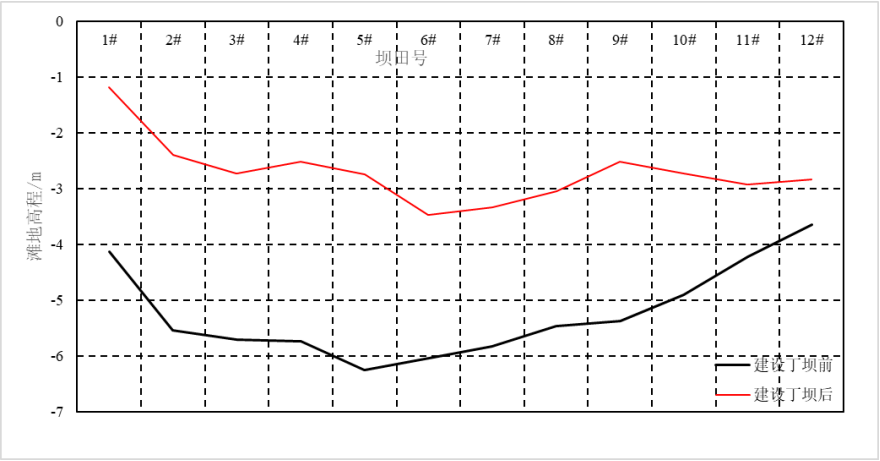

(b)Topographic changes before and after the construction of spur dikes

Fig. 12 Location of spur dikes and topographic changes before and after the construction of spur dikes

Table 3. Statistical table of elevation Changes at the lowest point of the beach within 10 meters in front of the seawall before and after the construction of spur dikes(m).

Scheme / Spur dikes	Before	After	Change
1#	-4.13	-1.18	2.98
2#	-5.55	-2.40	3.22
3#	-5.71	-2.73	3.51
4#	-5.74	-2.52	2.57
5#	-6.25	-2.74	2.50
6#	-6.04	-3.47	2.42
7#	-5.83	-3.33	2.87
8#	-5.47	-3.05	2.18
9#	-5.38	-2.51	1.31
10#	-4.91	-2.73	0.82
11#	-4.23	-2.92	2.95
12#	-3.65	-2.83	3.15

4 CONCLUSIONS

The dynamic characteristics of tidal bores are different from general river flow, which has strong turbulent mass waves and large velocity tidal currents. It causes serious riverbed erosion at the foot of the seawall. In tidal bore environments, spur dikes play a significant role in protecting the beach and the seawalls. In order to reduce the erosion harm of tidal bores over spur dikes, spur dikes under tidal bores are generally dominated by the low elevation of spur dikes to prevent tidal bore from directly scouring towards the foot of the seawall. By reducing the velocity of tidal currents in front of the seawall, a backflow in the middle area between dikes is formed. It is conductive to promote sediment deposition and make the beach elevated.

Spur dikes are designed with a length of 80 m, an interval space of 200 m and an elevation of 1.0 m (low elevation, about 1 m below the high tidal level). When encountering a 300 return year condition, the maximum and average flood velocity at the toe of the seawall is reduced by 70% and 56%, respectively, and the average ebb velocity is reduced by about 64%. The flow velocity in 60% of the middle area between dikes has decreased to below 1 m/s, and the circulation in the middle area between dikes is obvious. The elevation of the beach is above 1.0 m, which is higher than -4.0 m and satisfies the safety requirements of the seawall.

In the tidal bore environment, the flow around the head of spur dikes causes significant erosion holes in the area of the head of spur dikes. The effect of tidal bores over the spur dikes results in significant erosion of the beach at the upstream of the dikes. It should pay attention to the phenomenon and take protective measures in the macro-tidal estuary.

REFERENCES

Cheng Shuai. Research on the flow characteristics of spur dikes in curved river embankments. Three Gorges University, 2021.

Han Yufan. Research on the Bedding Effect of spur dikes. Nanjing Institute of Hydraulic Science, 2003.

Ren Yun, Zhang Gongjin, Lu Chuanteng. Study of flow structure around spur dike in bi-directional tidal flows. Yangtze River, 2017, 48(06):33-37.

Wang Renchao, Zhang Gongjin, Hu Caixia, Liu Rui, Wu Dongdong. Research on the Influence of Tidal Estuary Dike Layout on River Bed Scour. Pearl River, 2020, 41(01):63-68.

Wei Wenli, Chen Xiaopeng, Li Qiang, Zhang Zewei, Liu Yuling. Numerical simulation study on the influence of spur dikes on the hydraulic characteristics of bends. Journal of Water Resources and Water Engineering, 2019, 30(03):146-152.

Experimental study on the influence of reciprocating flow and unidirectional flow on sedimentation between dikes. Chinese Society of Marine Engineering. Proceedings of the 19th China Marine (Coastal) Engineering Academic Symposium, 2019:6.